These UC-MPC properties result in (i) better system performance (i.e., lower BER), (ii) higher difference between AC and CC values, (iii) easier decode in the receiver, and (iv) being a more efficient code sequence in asynchronous systems.

REFERENCES

1. G.C. Yang and W.C. Kwong, prime codes with applications to CDMA optical and wireless networks, Artech House Publishers, Norwood, MA, 2002.
2. H.M.H. Shalaby, Cochannel interference reduction in optical PPM-CDMA systems, IEEE Trans Commun 46 (1998) 799–805.
3. H.M.H. Shalaby, Complexities, error probabilities, and capacities of optical OOK-CDMA communication systems, IEEE Trans Commun 50 (2002) 2009–2017.
4. F. Liu, M. Karbassian and H. Ghafouri-Shiraz, Novel family of prime codes for synchronous optical CDMA, Opt Quant Electron 39 (2007) 79–90.
5. M.M. Karbassian and H. Ghafouri-Shiraz, Performance analysis of heterodyne-detected coherent optical CDMA using a novel prime code family, J Lightwave Technol 25 (2007) 3028–3034.
6. M.M. Karbassian and H. Ghafouri-Shiraz, IP routing and transmission analysis in optical CDMA networks: coherent modulation with incoherent demodulation, J Lightwave Technol 27 (2009) 3845–3852.
7. M.M. Karbassian and H. Ghafouri-Shiraz, Novel channel interference reduction in optical synchronous FSK-CDMA network using a data-free reference, J Lightwave Technol 26 (2008) 977–985.
8. M.M. Karbassian and H. Ghafouri-Shiraz, IP routing and traffic analysis in coherent optical CDMA networks, J Lightwave Technol 27 (2009) 1262–1268.

© 2012 Wiley Periodicals, Inc.

GUIDING TERAHERTZ WAVE WITHIN A LINE DEFECT OF PHOTONIC CRYSTAL SLAB

Lei Rao,[1] Dongxiao Yang,[1,2] and Zhi Hong[3]

[1] Department of Information and Electronic Engineering, Zhejiang University, Hangzhou 310027, People's Republic of China; Corresponding author: yangdx@zju.edu.cn

[2] Research Center for Terahertz Technology, Zhejiang University, Hangzhou 310027, People's Republic of China

[3] Centre for THz Research, China Jiliang University, Hangzhou 310018, People's Republic of China

Received 31 March 2012

ABSTRACT: *A terahertz line-defect waveguide in photonic crystal with a triangular lattice array of cylindrical air holes was fabricated on a silicon slab. Terahertz transmission spectra through this sample were measured and the waveguide with high transmittance exceeding 80% near 0.26 THz was experimentally obtained.* © 2012 Wiley Periodicals, Inc. Microwave Opt Technol Lett 54:2856–2858, 2012; View this article online at wileyonlinelibrary.com. DOI 10.1002/mop.27203

Key words: *terahertz; photonic crystals; waveguide; slab*

1. INTRODUCTION

''Terahertz (THz) gap,'' which usually refers to the frequencies from 0.1 to 10 THz, has attracted many attentions for its unique applications in the fields of imaging, detection, and communication [1]. Recent years, THz researches almost depend on free space device systems as solid-state platforms are still in the study [2]. Therefore, THz components such as waveguide are preferable to build up integrated solid-state platform for THz system. As photonic crystal, where the refractive index changes periodically along one- , two- , or three-dimensional directions was proposed, it has presented exciting manipulation of photons and received keen interest from many fields [3]. A variety of photonic crystal structures have been vigorously researched at THz regime, including filters, waveguides, and cavities [4–6]. The waveguide modes within the photonic band gap can actively propagate along the line defect of the photonic crystal waveguide. These waveguide modes can exhibit near-zero reflections and low losses through straight or even sharp bend [7], which will be applicable in the integrated THz devices.

In this article, a photonic crystal waveguide on high-resistivity silicon slab was fabricated by laser micromachining technology. The refractive index of the high-resistivity silicon slab and the transmission spectra of the photonic crystal waveguide were measured by a standard THz time-domain spectroscopy (THz-TDS) system and a submillimeter spectrum system, respectively. Experimental results show that there is a high transmittance of the photonic crystal waveguide sample in frequencies ranging from 0.26 to 0.268 THz. Calculated band diagram of the photonic crystal waveguide is in agreement with the experimental results.

2. SIMULATION

The whole THz-TDS system was fulfilled with nitrogen to decrease the relative humidity to almost zero during the measurement for refractive index of high-resistivity silicon slab used in the fabrication of photonic crystal waveguide sample. The output time-domain waveform of THz pulse through a high-resistivity silicon slab along thickness direction was recorded. The reference signal was the time-domain waveform of the THz pulse without the silicon slab sample. The refractive index spectrum of the high-resistivity silicon slab is extracted from the phase of the transmission coefficient [8], as shown in Figure 1.

From 0.2 to 0.6 THz in Figure 1, the refractive index increases sharply, whereas from 0.6 to 1.6 THz, the refractive index of silicon increases almost linearly. At frequencies higher than 1.6 THz, the refractive index drops slightly. This is because that the intensities are weak at the edges of the reference THz spectrum lower than 0.6 THz and higher than 1.6 THz. Hence, the measured error is introduced in the refractive index at these frequency ranges. The refractive index from 0.6 to 1.6 THz can be fit by a linear line, as shown by the red line in Figure 1.

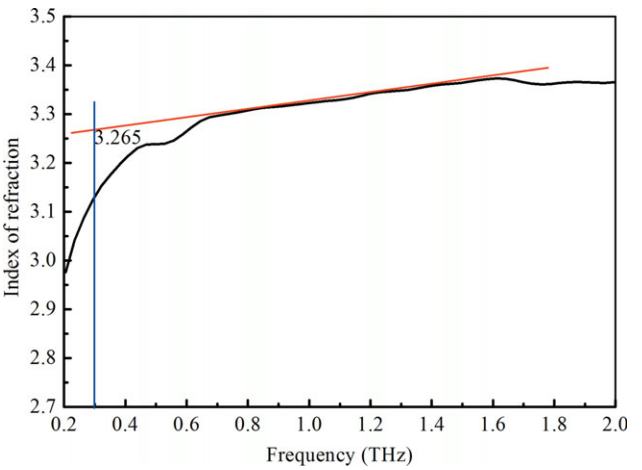

Figure 1 Measured refractive index of high-resistivity silicon. [Color figure can be viewed in the online issue, which is available at wileyonlinelibrary.com]

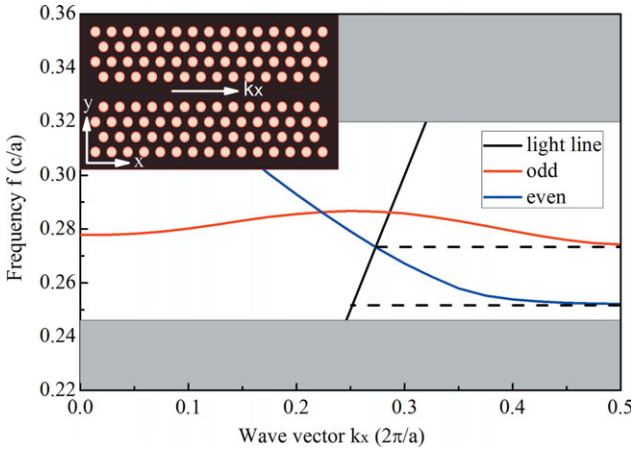

Figure 2 Band diagram of TE-like modes for the photonic crystal waveguide along Γ-K direction. The inset shows the schematic diagram of the photonic crystal waveguide. [Color figure can be viewed in the online issue, which is available at wileyonlinelibrary.com]

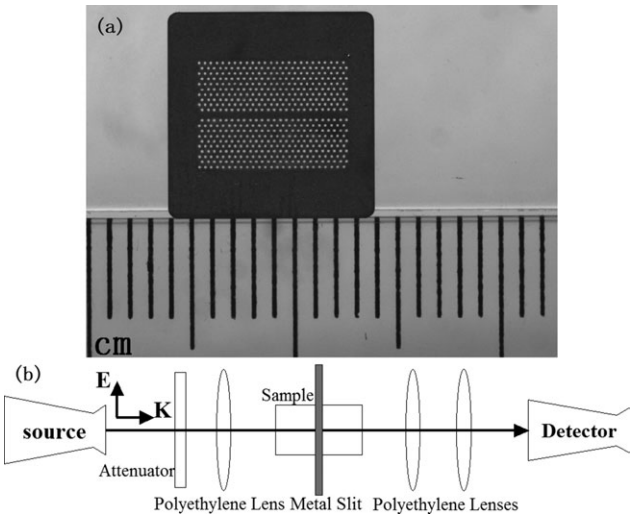

Figure 3 (a) Specimen of the photonic crystal waveguide. (b) Schematic of submillimeter spectrum system setup

It can be calculated by linear interpolation method that the refractive index of silicon at 0.3 THz is 3.265 as indicated by the blue line, which is slightly smaller than previous results [9]. The differences of sample material and frequency ranges may be the explanation of this discrepancy.

A terahertz line-defect waveguide in photonic crystal with a triangular lattice array of cylindrical air holes on silicon is shown in the inset of Figure 2. The structure parameters of the photonic crystal waveguide are as follows: triangular lattice constant a, slab thickness a, and air hole radius $0.3a$. The slab material is high-resistivity silicon with the measured refractive index of 3.265. The band diagram of the photonic crystal waveguide was calculated by the three-dimensional finite difference time domain (FDTD) method [10]. The band diagram of TE-like (electric field is parallel with the slab plane) modes for the photonic crystal waveguide along Γ-K direction with normalized frequency (c/a) is shown in Figure 2. The black line is the light line, below which the EM waves can be restricted to transmit within the slab. The gray shadows are the leaky regions, where EM waves can be extended into the photonic crystal. It can be found that there are two waveguide modes with even and odd symmetries appearing within the band gap, respectively. Below the light line, both the two waveguide modes are confined horizontally by the band gap and vertically by the index guiding. Therefore, the EM waves of these two waveguide modes are restricted to propagate within the line-defect and should be lossless in an ideal photonic crystal waveguide without imperfections [11]. As indicated by the dash lines, a single mode with even symmetry exists below the light line and its frequency range is from 0.252 (c/a) to 0.273 (c/a). Parts of the waveguide modes existing above the light line can be extended into the air, which will bring large out-of-plane radiation loss.

3. EXPERIMENT

A photonic crystal waveguide specimen whose structure is the same as that in the simulation is shown in Figure 3(a). Its lattice constant and area are 290 μm and 10 mm by 10 mm, respectively. Triangular lattice array of cylindrical air holes was fabricated on the high-resistivity silicon slab and the waveguide was formed by line-defect of air holes along the Γ-K direction. The transmission spectra of the photonic crystal waveguide were measured by a submillimeter spectrum system which includes THz backward wave oscillator (BWO) and pyroelectric detector. The Schematic of experimental setup of submillimeter spectrum system is shown in Figure 3(b). THz waves with electric field polarization in the plane of the slab (TE modes) and frequencies from 0.23 to 0.37 THz were emitted from BWO with the frequency step of 300 MHz. The photonic crystal waveguide sample was placed in the middle of two high-density polyethylene lenses which were used to couple THz waves into the slab and to collimate THz waves from the slab, respectively. Metal slit was added in the middle of the photonic crystal waveguide sample to block the EM waves which did not transmit through the slab and emit into the air. The transmitted beam was focused by the third high-density polyethylene lens and detected by high-

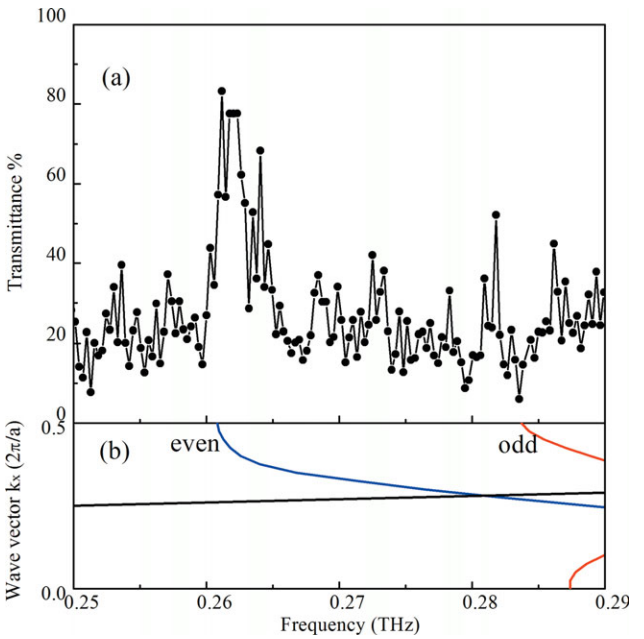

Figure 4 (a) Transmittance spectrum of the photonic crystal waveguide sample measured by submillimeter spectrum system. (b) Redraw of Figure 2 with the lattice constant of 290 μm. [Color figure can be viewed in the online issue, which is available at wileyonlinelibrary.com]

sensitive pyroelectric detector. The transmission spectra of both the photonic crystal waveguide sample and a reference silicon slab with the same size were measured by this submillimeter spectrum system.

Figure 4(a) shows the transmittance spectrum of the photonic crystal waveguide sample, which is defined as the transmission spectrum of the sample dividing that of the silicon slab. The calculated band diagram of the photonic crystal waveguide with the lattice constant of 290 μm in Figure 2 is redrawn in Figure 4(b) to give a comparison with the experimental results. The transmittance is low from 0.25 to 0.26 THz as no waveguide modes can support the EM waves propagation, while it increases significantly from 0.26 to 0.268 THz due to the appearance of the even waveguide mode in band diagram of the photonic crystal waveguide. It should be point out that the sharp peaks in the measured spectra of samples are caused by the BWO. As frequency increases further, the transmittance decreases because the waveguide mode approaches to the light line. The fabrication errors can cause the EM waves of the waveguide mode near the light line coupled into the air and increase the radiation loss. In addition, the large impedance mismatch between the small group velocity of the waveguide mode in the photonic crystal waveguide and the EM wave velocity in the free space will also bring coupling loss [12].

4. CONCLUSION

Transmission power measurements of a photonic crystal waveguide sample in the frequency range from 0.23 to 0.37 THz reveal that a comparably low propagation loss and high transmittance near 0.26 THz can be achieved. Unavoidable fabrication flaws can increase propagation loss, especially for the EM waves of waveguide mode near the light line. Nevertheless, the photonic crystal waveguide effect promising the high transmittance near 0.26 THz is fulfilled in our experiments. This kind of photonic crystal waveguide may open up the way to exploitation of THz-integrated solid-state platforms.

ACKNOWLEDGMENTS

This work was supported by the National Natural Science Foundation of China (NSFC) under Grant Nos. 60671006 and 60971059.

REFERENCES

1. I. Hosako, N. Sekine, M. Patrashin, S. Saito, K. Fukunaga, Y. Kasai, P. Baron, T. Seta, J. Mendrok, S. Ochiai, and H. Yasuda, At the dawn of a new era in terahertz technology, Proc IEEE 95 (2007), 1611–1623.
2. H. Page, S. Malik, M. Evans, I. Gregory, I. Farrrer, and D. Ritchie, Waveguide coupled terahertz photoconductive antennas: Toward integrated photonic terahertz devices, Appl Phys Lett 92 (2008), 163502, 1–3.
3. S. Noda, Recent progresses and future prospects of two- and three-dimensional photonic crystals, J Lightwave Technol 24 (2006), 4554–4567
4. K. Takagi and A. Kawasaki, Fabrication of three-dimensional terahertz photonic crystals with diamond structure by particle manipulation assembly, Appl Phys Lett 94 (2009), 021110–021110–3.
5. A.L. Bingham and D.R. Grischkowsky, Terahertz 2-D photonic crystal waveguides, IEEE Microwave Wireless Compon Lett 18 (2008), 428–430.
6. C.M. Yee and M.S. Sherwin, High-Q terahertz microcavities in silicon photonic crystal slabs, Appl Phys Lett 94 (2009), 154104, 1–3.
7. J.D. Joannopoulos, S.G. Johnson, J.N. Winn, and R.D. Meade, Photonic crystals: molding the flow of light, 2nd ed., Princeton University Press, 2008.
8. T.D. Dorney, R.G. Baraniuk, and D.M. Mittleman, Material parameter estimation with terahertz time-domain spectroscopy, J Opt Soc Am A, 18 (2001), 1562–1571.
9. E.D. Palik, Handbook of optical constants of solids, Academic Press, 1985.
10. A.F. Oskooi, D. Roundy, M. Ibanescu, P. Bermel, J.D. Joannopoulos, and S.G. Johnson, MEEP: A flexible free-software package for electromagnetic simulations by the FDTD method, Comput Phys Commun 181 (2010), 687–702.
11. A. Baron, S. Mazoyer, W. Smigaj, and P. Lalanne, Attenuation coefficient of single-mode periodic waveguides, Phys Rev Lett 107 (2011), 153901, 1–5.
12. S.J. Mcnab, N. Moll, and Y.A. Vlasov, Ultra-low loss photonic integrated circuit with membrane-type photonic crystal waveguides, Opt Express 11 (2003), 2927–2939.

© 2012 Wiley Periodicals, Inc.

A MODULAR APPROACH TO DESIGN A FULL THREE-WAY 8 TO 18 GHz MMIC ACTIVE CIRCULATOR

Hong Yi Lim,[1] Geok Ing Ng,[1] Kian Sen Ang,[2] and Yoke Choy Leong[2]

[1] Nanyang Technological University, Singapore, 50 Nanyang Avenue, Singapore 639798

[2] DSO National Laboratories, 20 Science Park Drive, Singapore 118230; Corresponding author: limh0115@ntu.edu.sg

Received 3 April 2012

ABSTRACT: *A modular approach to design full three-way active circulator is presented. Derived S-parameters for the modular design approach illustrates that broadband performance can be achieved with broadband performance modules. A full three-way 8 to 18 GHz MMIC active circulator was designed and fabricated with broadband feedback amplifiers and broadband 180° hybrids.* © 2012 Wiley Periodicals, Inc.

Microwave Opt Technol Lett 54:2858–2861, 2012; View this article online at wileyonlinelibrary.com. DOI 10.1002/mop.27202

Key words: *active circulator; circulator; microwave monolithic integrated circuits; 180° hybrids*

1. INTRODUCTION

A microwave circulator is a three-port device that permits microwave signals to propagate in a particular direction, for example, clockwise direction, from one of the ports to the adjacent port and prohibits the transmission of microwave signals in the opposite direction. This property of directivity with single transmission direction and complete isolation in the opposing direction is illustrated in the *S*-parameters for an ideal circulator [1] shown in Figure 1.

A circulator is an important microwave component used in many microwave system such as reflection phase shifters and in T/R modules to isolate the transmitted and received signal. Most circulators are made of magnetic ferrite materials which makes it hard for MMIC integration. Consequently, an active circulator

Figure 1 *S*-parameters for an ideal circulator